



ELSEVIER

Polymer 34 (2002) 6661–6667

polymerwww.elsevier.com/locate/polymer

Phase behaviour of SMMA and SAN blends using Flory's equation of state theory

P. Tang^a, G.X. Li^a, J.S. Higgins^{b,*}, V. Arrighi^c, J.T. Cabral^b^aDepartment of Polymer Materials Science and Engineering, Sichuan University, Chengdu 610065, People's Republic of China^bDepartment of Chemical Engineering and Chemical Technology, Imperial College of Science, Technology and Medicine, Prince Consort Road, London SW7 2BY, UK^cDepartment of Chemistry, Heriot-Watt University, Edinburgh EH14 4AS, UK

Received 14 March 2002; accepted 21 August 2002

Abstract

The thermodynamic phase behaviour of blends composed of two random copolymers of polystyrene-*co*-methyl methacrylate (SMMA) and polystyrene-*co*-acrylonitrile (SAN) was studied using a modified Flory's equation of state (EOS) theory. Light scattering measurements indicated that SMMA and SAN are miscible within certain copolymer composition ranges and exhibit lower critical solution temperature behaviour. The temperature, at which phase separation is observed, changes with the copolymer composition. The segmental interaction energy parameters X_{S-MMA} , X_{S-AN} and X_{MMA-AN} were calculated using a binary interaction model by fitting the lowest temperature in the calculated spinodal boundary from EOS theory to the experimental data for several copolymer compositions. It was found that EOS theory, originally used for binary polymer solutions, could be modified and successfully extended to simulate the phase boundaries of random copolymer blends, when using Flory's mixing rule to calculate the equation of state parameters for the copolymers from those of the constituent monomer segments. © 2002 Elsevier Science Ltd. All rights reserved.

Keywords: Copolymers; Polymer blends; Equation of state theory

1. Introduction

Blending of existing polymers has now become a common method used to produce materials with new or improved properties compared to those of its constituents. However, the number of miscible homopolymer pairs is quite limited due to the generally unfavourable mixing enthalpy between different monomer species and to the low combinatorial entropy associated with mixing of the two high molecular weight polymers. Addition of a copolymer has been known to improve miscibility between polymer blend components. Over the past two decades, extensive studies of the miscibility window behaviour in blends containing random copolymers have been carried out [1–8]. These studies are of technological interest: the synthesis of random copolymers is relative inexpensive compared to the preparation of block copolymers and therefore these materials can be used in large-scale industrial processes.

A homopolymer might form a miscible blend with a copolymer in certain copolymer composition and temperature ranges, even if all segmental interactions are positive (and therefore unfavourable to mixing). The driving force for the miscibility resides in the so-called 'intramolecular repulsive interaction' which exists between the components of the same copolymer chain [1–3]. This provides an alternative route to the establishment of a negative X_{blend} for blends containing random copolymers. One typical example is the blend of poly(methyl methacrylate) (PMMA)/polystyrene-*co*-acrylonitrile (SAN). Although PMMA is not miscible with either polyacrylonitrile (PAN) or polystyrene (PS), miscible blends can be prepared with SAN copolymers of limited AN content [9,10]. Within the miscibility boundaries, the PMMA/SAN blends exhibit lower critical solution temperature (LCST) behaviour, in which phase separation occurs upon heating [11–16]. To date, most of the theoretical work on polymer blends comprising at least one copolymer has been carried out using Flory–Huggins mean-field theory, mainly because of its extreme simplicity. However, it is well known that the

* Corresponding author. Tel.: +44-207-594-5565; fax: +44-207-594-5638.

E-mail address: j.higgins@ic.ac.uk (J.S. Higgins).

Table 1
Characteristics of the copolymers investigated

Polymer	Molecular weight (M_w)	DPI (M_w/M_n)	T_g^a (°C)	Refractive index ^b	Copolymer composition (S vol%)	Source
SMMA40	122,500	2.0	111	1.5284	40	Synthesized in the lab
SMMA40S	55,760	1.8	107	1.5254	37	Synthesized in the lab
SMMA8	57,650	1.6	122	1.4956	8	Synthesized in the lab
SMMA30	66,700	1.8	112	1.5151	27	Synthesized in the lab
SAN87	371,000	1.8	97	1.5276	87	Synthesized in the lab
SAN83	349,800	1.8	106	1.5302	83	Synthesized in the lab
SAN75	150,000	2.2	113	1.5720	75	Aldrich
SAN70	137,000	2.4	115	1.5684	70	Aldrich

^a T_g s were obtained using a Perkin–Elmer Pyris 1 at a scanning rate of 20 K/min.

^b Refractive indices are interpolated from data of PMMA, PS and PAN using appropriate weight fractions.

traditional Flory–Huggins (F–H) model does not explain, even qualitatively, many of the most important thermodynamic features of polymer blends, such as the LCST behaviour. In order to overcome this drawback of the original F–H theory, Flory’s equation of state (EOS) theory introducing the free volume effect on the entropy and enthalpy of mixing was used to understand quantitatively both the LCST and UCST behaviour of polymer blends [17–22]. This model has been able to predict successfully the phase behaviour of binary systems comprising copolymers mixed with homopolymers [23–28]. To date, however, there is a shortage of investigations dealing with the phase behaviour of blends of two copolymers.

In this paper we present a light scattering study of the phase behaviour of polystyrene-*co*-methyl methacrylate (SMMA)/SAN blends as a function of copolymer composition and temperature. The experimental data are compared to the calculated spinodal curves with X_{ij} obtained from fitting the calculated phase diagrams to the experimental ones on the basis of a modified EOS theory.

2. Theory

Using the notation of Flory and his collaborators [29–31], the equation of state for pure polymers as well as polymer blends is given by

$$\frac{\tilde{p}_i \tilde{v}_i}{\tilde{T}_i} = \frac{\tilde{v}_i^{1/3}}{\tilde{v}_i^{1/3} - 1} - \frac{1}{\tilde{v}_i \tilde{T}_i} \quad (1)$$

where $\tilde{p}_i = p/p_i^*$, $\tilde{v} = v_i/v_i^*$, and $\tilde{T} = T_i/T_i^*$ are the reduced pressure, volume and temperature, respectively, and the p_i^* , v_i^* and T_i^* are the equation of state or characteristic parameters of component i , which are constant for any given polymer species. \tilde{v}_i and p_i^* are obtained from the thermal expansion coefficient and the thermal pressure coefficient, respectively, whereby T_i^* is derived from Eq. (1).

For a binary blend, the spinodal is defined by the

following relationship [21]:

$$\partial \Delta^2 G_m / \partial \Phi_2^2 = 0 \quad (2)$$

namely,

$$\begin{aligned} & -\frac{1}{\Phi_1} + \left(1 - \frac{r_1}{r_2}\right) - \frac{p_1^* V_1^*}{RT_1^*} \frac{\partial \tilde{v}}{\partial \Phi_2} \frac{1}{\tilde{v} - \tilde{v}^{2/3}} \\ & + \frac{p_1^* V_1^*}{RT_{sp}} \frac{1}{\tilde{v}^2} \frac{\partial \tilde{v}}{\partial \Phi_2} + \frac{V_1^* X_{12}}{RT_{sp}} \frac{2\Phi_2}{\tilde{v}} - \frac{V_1^* X_{12}}{RT_{sp}} \frac{\Phi_2^2}{\tilde{v}^2} \frac{\partial \tilde{v}}{\partial \Phi_2} \\ & = 0. \end{aligned} \quad (3)$$

Note that Eq. (3) neglects both the effect of pressure and molecular weight distribution on the phase diagram. The literature research results showed that the binodal is greatly affected by the polydispersity whereas the spinodal is not [17,21]. Furthermore, the copolymers used in this study are not very polydisperse as seen in Table 1, and hence using Eq. (3) to calculate the spinodal boundary is reasonable. In Eq. (3), r_i is segmental fraction of component i , V_i^* is molar characteristic volume of component i , \tilde{v} the reduced volume of the blend, knowing that \tilde{p} and \tilde{T} , which are given

$$\tilde{p} = p/p^* = \Phi_1 p_1^* + \Phi_2 p_2^* - \Phi_1 \theta_2 X_{12} \quad (4)$$

$$\tilde{T} = \frac{p_1^* \tilde{T}_1 \Phi_1 + p_2^* \tilde{T}_2 \Phi_2}{\Phi_1 p_1^* + \Phi_2 p_2^* - \Phi_1 \theta_2 X_{12}} \quad (5)$$

and hence \tilde{v} can be determined from Eq. (1). The parameter θ_i represents the site fraction

$$\theta_i = s_i / (s_1 \Phi_1 + s_2 \Phi_2) \quad (6)$$

where s_i is the segmental contact area, which can be obtained from Bondi’s method [32]. Characteristic parameters for the copolymer 1 ($A_x B_{(1-x)}$) can be evaluated from the usual combining or mixing rules [23]:

$$p_1^* = x p_A^* + (1-x) p_B^* - x(1-x) X_{AB} \quad (7)$$

$$1/T_1^* = (x p_A^*/T_A^* + (1-x) p_B^*/T_B^*)/p_1^* \quad (8)$$

$$\theta_A = 1 - \theta_B = \frac{s_A x}{s_A x + s_B(1-x)} = \frac{x}{x + \frac{s_B}{s_A}(1-x)} \quad (9)$$

According to Flory's binary interaction model based on the assumption of random mixing [23,25], the interaction parameter X_{blend} between copolymer 1 ($A_x B_{1-x}$) and copolymer 2 ($C_y D_{1-y}$) is given by

$$X_{\text{blend}} = x\theta_C X_{AC} + x\theta_D X_{AD} + (1-x)\theta_C X_{BC} + (1-x)\theta_D X_{BD} - x\theta_B X_{AB} - (s_1/s_2)y\theta_D X_{CD} \quad (10)$$

where x and y are the volume fraction of A and C in the $A_x B_{1-x}$ and $C_y D_{1-y}$ copolymers, respectively.

3. Experimental

3.1. Materials

Copolymers of SMMA and SAN were synthesised by free radical polymerisation in toluene solution for 3–4 h at 343 K using AIBN as initiator. The monomers, i.e. styrene and MMA purchased from Aldrich, were freed from inhibitor and distilled prior to use. The resulting polymer solutions were precipitated into a large excess of methanol, purified and then dried in vacuum for over one week. The degree of conversion was kept below 30% in order to avoid copolymer composition drifts.

The molecular weights of SMMA and SAN samples were estimated by gel permeation chromatography (GPC) using polystyrene standards from Rapra Technology Ltd. The composition of SMMA was determined by ^1H NMR.

3.2. Preparation of blends

For light scattering experiments, copolymer blends of SMMA and SAN were prepared at various weight fractions by solution casting from THF (5% w/v). The solutions were cast on a 16 mm diameter microscope glass cover slip and kept at room temperature for one day in order to evaporate the solvent slowly. The samples were then further dried in a vacuum oven in which the temperature was raised gradually until at least 20 K above the glass transition temperatures of the blend during a period of ca. 2 weeks.

3.3. Light scattering measurements

The cloud points of SAN/SMMA were measured using a home-built light scattering apparatus for which details of design have been described elsewhere [36,37]. A He–Ne laser of 633 nm wavelength is directed onto the sample and the scattered light detected by an array of 32 photo-diodes aligned above the sample in an arc from 5 to 67°.

4. Results and discussion

4.1. Cloud point curves of SMMA/SAN

In a homogeneous system, the refractive index is uniform throughout and, hence, light can pass through unaffected. As a blend undergoes phase separation, however, light scattering results from the variation of the refractive index in the sample, provided that there is a reasonable difference between the refractive indices of the components and that the size of the dispersed phase is comparable to the wavelength of light. Values of the refractive indices of SAN and SMMA listed in Table 1, suggest that light scattering is a suitable technique for detecting the phase separation of this system.

In this work, the copolymer systems selected for light scattering measurements, e.g. as SMMA8/SAN75 and SMMA30/SAN75, formed transparent films at room temperature. To determine the cloud points of the SMMA/SAN blends, a series of light scattering measurements were carried out as a function of heating rate. As shown in Fig. 1, the cloud point coincides with the temperature at which a sudden increase in the intensity of scattered light is observed. Due to the viscous and highly entangled nature of polymeric materials, values of cloud point temperature (T_c) depend upon heating rate. T_c increases with increasing heating rate and, consequently, the intensity change detected does not represent the true phase boundary.

To overcome this problem, in this work, we carried out measurements at three different heating rates: 0.2, 0.5 and 1 K/min. Phase boundary temperatures corresponding to zero heating rate were determined by extrapolation, as shown in Fig. 2 for samples with different blend ratios. In a few cases only two heating rates were used because SMMA and SAN degrade at high temperature, especially if held there for long time, and, as a consequence, the cloud point

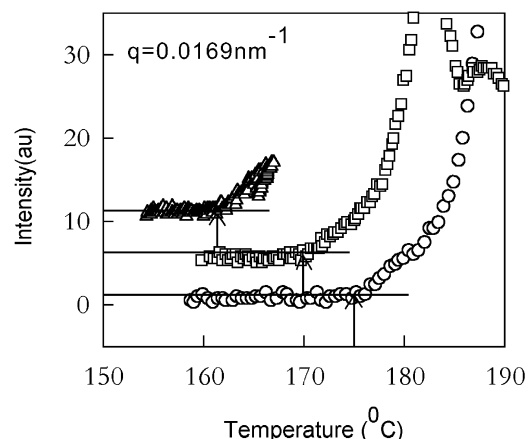
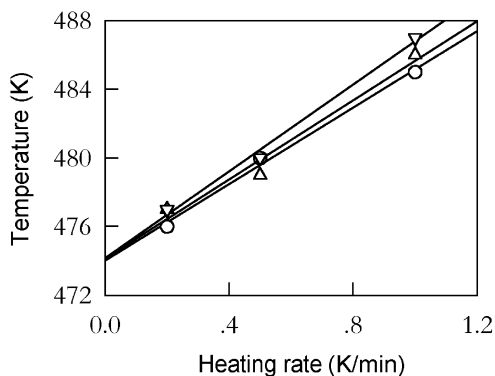
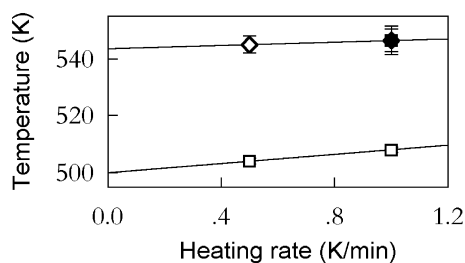


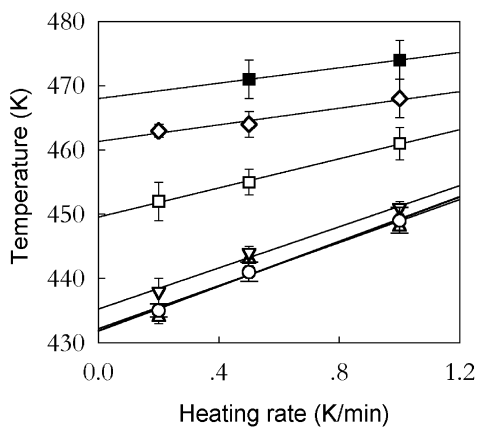
Fig. 1. Dependence of cloud point temperatures on heating rate for a SMMA30/SAN75 (50/50) blend. T_c values are marked by arrows and values of heating rates are reported: (Δ) 0.2 K/min; (\square) 0.5 K/min, (\circ) 1.0 K/min.



(a) SMMA8/SAN75



(b) SMMA8/SAN75



(c) SMMA30/SAN75

Fig. 2. Cloud point temperatures as a function of heating rate for (a) SMMA8/SAN75: (∇) 80/20, (\circ) 60/40, (Δ) 50/50; (b) SMMA8/SAN75: (\blacksquare) 85/15, (\square) 30/70, (\diamond) 20/80; (c) SMMA30/SAN75: (\blacksquare) 85/15, (∇) 80/20, (\circ) 60/40, (Δ) 50/50, (\square) 30/70, (\diamond) 20/80. The lines indicate extrapolation to zero heating rate. In (a) cloud point temperatures are reported without showing error bars, for clarity.

temperatures could not be detected for the lowest heating rate. In Fig. 2(a), cloud point temperatures are reported for a series of SMMA8/SAN75 (80/20, 60/40 and 50/50) and, for clarity of presentation we do not show the corresponding errors. The large error bars for the sample with 15% SAN (Fig. 2(b)) and for the 10% SAN blend (Fig. 2(c)) indicate that the phase transition temperature could not be detected precisely at these particular compositions. One of the reasons for this may be due to the very high phase separation

temperature at which the blends would degrade. That is why only two heating rates of 0.5 and 1.0 K/min were used for light scattering measurements at these particular compositions. The slope of the apparent cloud point temperatures vs. heating rate curve is seen to be somewhat steeper for those compositions, which phase separate at lower temperatures. This is probably, due to the very slow response of these high molecular weight systems when the temperature lowers towards the glass transition. However, the stronger heating rate effect observed in this work is attributed to the molecular weight of SAN used in this experiment.

4.2. Calculation of phase boundary

As mentioned in Section 2, in order to evaluate thermodynamic quantities for binary system, we need to determine values of the characteristic parameters, e.g. v_i^* , p_i^* and T_i^* for the respective copolymers. In this paper, we assumed that the characteristic parameters of the monomers in copolymers are equal to those of the corresponding homopolymers. Values of the characteristic parameters are taken from Won Ho Jo's study [25] and these are listed in Table 2.

In addition to the parameters mentioned above, the binary segmental interaction energy parameters X_{ij} are also required in order to calculate phase boundaries. For low molecular weight analogues, X_{ij} can be obtained from measurements of heat of mixing. However, it has been shown that X_{ij} values obtained from this method are generally too large [21]. In this paper, values of X_{ij} were obtained by fitting the calculated phase diagrams derived from EOS theory to the experimental data under the assumption that the minimum of the cloud point temperature coincides with the critical temperature of the phase diagram. Once X_{blend} is known for several of copolymer compositions, we can calculate X_{ij} using the binary interaction model (Eq. (10)). The resulting segmental interaction energy parameters are $X_{\text{S-MMA}} = 3.4 \text{ J/cm}^3$, $X_{\text{MMA-AN}} = 25.4 \text{ J/cm}^3$, and $X_{\text{S-AN}} = 44.8 \text{ J/cm}^3$. There are only three values here unlike Eq. (10) since our copolymers are AB and BC containing the same comonomer.

Using the method introduced in Section 2, the spinodal curves were calculated using Eq. (3) and the X_{ij} values determined as described above. Numerical solutions of the spinodal equation for SMMA/SAN obtained by plotting the left side values of Eq. (3) as a function of SAN volume fraction at various spinodal temperatures, are shown in

Table 2
Characteristic parameters of the polymers used in this study

Polymer	v_{sp}^* (cm^3/g)	p^* (J/cm^3)	T^* (K)
PS	0.8466	453	8982
PMMA	0.7643	562	8474
PAN	0.7798	810	11,680

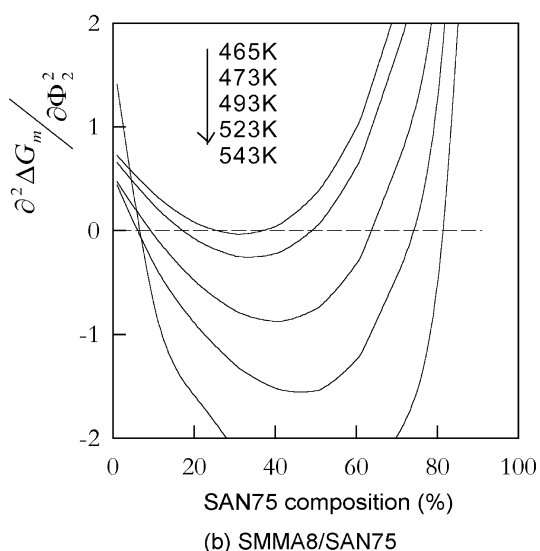
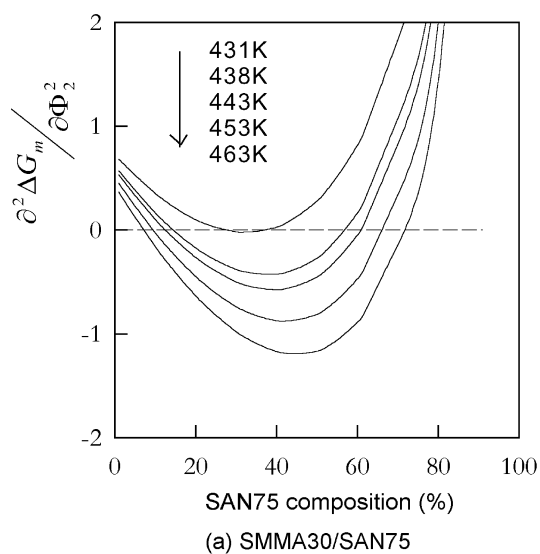


Fig. 3. Calculated $\partial^2 \Delta G_m / \partial \Phi_2^2$ versus SAN content, Φ_2 , at different temperatures. (a) SMMA30/SAN75 and (b) SMMA8/SAN75.

Fig. 3. For convenience, a horizontal dashed line representing the miscibility limit was drawn at $\partial^2 \Delta G_m / \partial \Phi_2^2 = 0$. The intersection of the $\partial^2 \Delta G_m / \partial \Phi_2^2$ curve and the horizontal dashed line represents the spinodal compositions at the corresponding spinodal temperatures. The resulting spinodal curves are reported in Fig. 4 together with the experimental cloud points.

These blends exhibit LCST behaviour within certain copolymer composition ranges, just as the case of a blend of PMMA/SAN as is observed from both calculations and experiment. According to EOS theory, there are three contributions influencing the miscibility of polymer blends [28]: a combinatorial entropy term, an interaction term and the free volume term. For the SMMA/SAN system, negative X_{blend} values between SMMA and SAN within a certain range of copolymer compositions are the main factor leading to LCST behaviour.

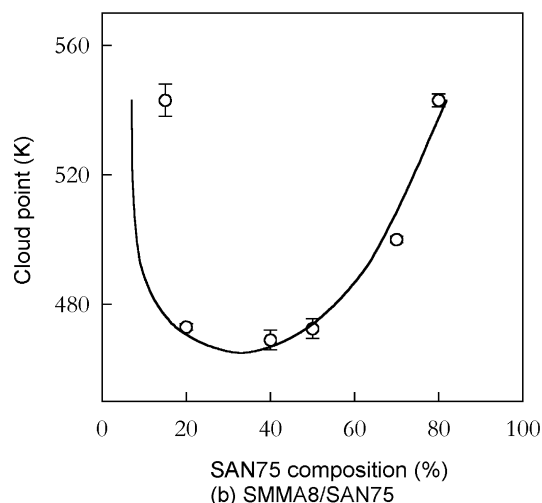
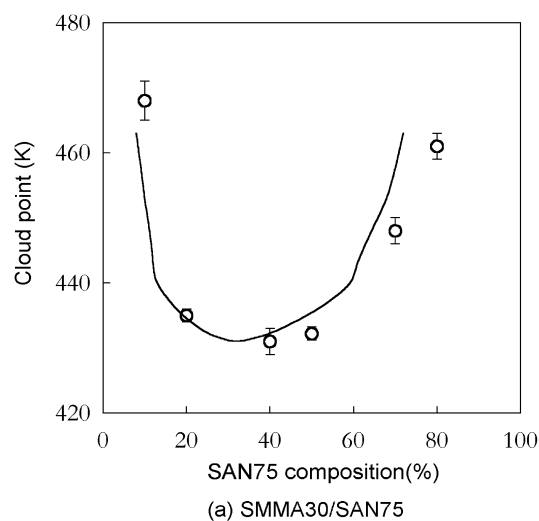


Fig. 4. Phase boundaries versus blend composition: (a) SMMA30/SAN75 and (b) SMMA8/SAN75. The symbols indicate the experimental cloud points extrapolated to zero heating rate whereas the solid lines are the calculated spinodal curves using data reported in Fig. 3.

As shown in Fig. 4, although the agreement between experimental data and theoretical calculations is very good, at low SAN content, the calculated spinodal temperatures are lower than the experimental cloud points extrapolated to zero heating rate. On the contrary, at higher SAN content, the calculated curves are higher than the experimental values. There are several possible reasons for this but mainly we have to note that for off critical blends, where there is a large metastable gap to pass through before the spinodal temperature is reached, the cloud points may represent something closer to the binodal temperature. This issue can be resolved by careful light scattering experiments during phase separation kinetics after a jump inside the spinodal [38].

Another possible reason for the discrepancy is that the characteristic parameters used for the monomers in the copolymers refer to literature data and these may differ from the experimental values. Furthermore, the simple mixing

rule, i.e. Eqs. (7)–(9), used to obtain the characteristic parameters for the copolymers may need to be modified, since, in some cases, deviations between calculations and experimental results have been found [28].

The phase separation temperature changes with copolymer compositions. For example, the LCST of SMMA8/SAN75 is higher than that of SMMA30/SAN75 (Fig. 4), due to the more negative X_{blend} between SMMA8 and SAN75. Comparing with the LCST of other blends, PMMA/SAN samples at the same SAN copolymer composition showed a higher LCST than SMMA/SAN because of the more negative X_{blend} values between PMMA and SAN, i.e. using SMMA instead of PMMA will decrease the LCST of the blend of PMMA/SAN.

4.3. Miscibility window

Since SMMA and SAN copolymers contain a common monomer, there are only three different interaction energy parameters, which are the same as those of a blend of PMMA and SAN. Ougizawa et al. [28] studied the phase behaviour of PMMA/SAN blends and reported the following X_{ij} values: $X_{S-MMA} = 3.4 \text{ J/cm}^3$, $X_{MMA-AN} = 24.9 \times \text{J/cm}^3$ and $X_{S-AN} = 45.1 \text{ J/cm}^3$. These values are very close but not identical to those we reported above from fitting data for our blends. It is interesting, therefore, using PMMA/SAN literature values, to calculate the miscibility window for our copolymer/copolymer blends based upon a binary interaction model. The results can then be compared to those obtained using calculated X_{ij} values, as explained earlier in this work. The miscibility window where $X_{\text{blend}} = 0$ (Eq. (10)) is described by a function of the copolymer composition x and y , and the solution can be readily obtained in the x – y plane. The enclosed area is the miscible area in Fig. 5. Visual inspection of the turbidity of the samples, as well as light scattering measurements, was employed to obtain the miscibility region experimentally.

The calculated miscible window is wider than the experimental one. Several factors may contribute to this discrepancy: (a) the segmental interaction parameters, X_{ij} are assumed to be composition- and temperature-independent; (b) both components are assumed to be randomly mixed, and hence the influence of sequence distribution of the copolymer on the miscibility is ignored. However, some literature results have shown that the sequence distribution of the copolymer will affect the charge distribution and the probability of contact between interaction sites and thereby affect the miscibility [33–35]; (c) Any free-volume contributions to the mixing process are neglected in Eq. (10) based upon the random mixing assumption. The X_{ij} obtained in this work from fitting the simulated phase diagram to the experimental data using Flory EOS theory, may solve this problem to some extent since this theory considers the free volume effect. However, the calculated X_{ij} obtained from fitting the data for the composition at the lowest temperature of the phase diagram should correspond

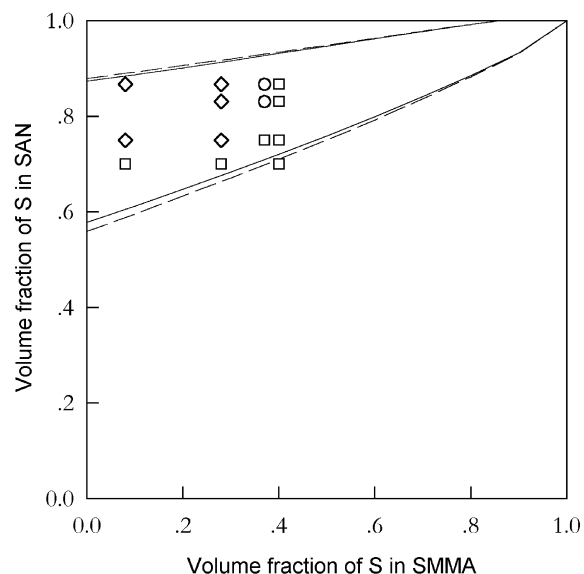


Fig. 5. Miscibility window of SMMA/SAN blends. The symbols represent experimental points: (□) immiscible blends, (◇) miscible blends and (○) partially miscible systems. The solid lines refer to calculations using literature X_{ij} values whereas the dashed lines represent calculated curves using values reported in this work.

to consideration of the free volume effect only at this particular composition, i.e. the changes of the free volume with blend composition are ignored. The X_{ij} values obtained in this way cannot therefore completely account for the effect of free volume on the miscibility at other blend compositions.

5. Conclusions

The results presented in this work demonstrate that blends containing two copolymers may be miscible within a certain copolymer composition range even where the corresponding homopolymers are immiscible. The phase boundary at different blend ratios was calculated as a function of temperature, based upon a modified Flory EOS theory. The required segment–segment interaction parameters X_{ij} and the EOS parameters for the copolymers were obtained from suitable mixing rules. The extent of the agreement between calculated phase boundaries and experimental data depends on the accuracy of the values of X_{ij} and EOS parameters used. The binary interaction model based upon the mean-field theory cannot completely account for the miscibility of the blends containing two copolymers.

Acknowledgements

The authors wish to acknowledge financial support from the Royal Society and National Natural Science Foundation in China. We thank Dr C. Rodrigues for assistance with

carrying out the NMR measurements to determine the copolymer compositions.

References

- [1] Brinke G, Karasz FE, MacKnight WJ. *Macromolecules* 1983;16:1827–32.
- [2] Paul DR, Barlow JW. *Polymer* 1984;25:487–94.
- [3] Kambour RP, Bendler JT, Bopp RC. *Macromolecules* 1983;16:753–7.
- [4] Fowler ME, Barlow JW, Paul DR. *Polymer* 1987;28:1177–84.
- [5] Shiomi T, Karasz FE, MacKnight WJ. *Macromolecules* 1986;19:2274–80.
- [6] Nishimoto N, Keskkula H, Paul DR. *Polymer* 1989;30:1279–86.
- [7] Cowie JMG, Reid VMC, McEwen IJ. *Polymer* 1990;31:486–9.
- [8] Suess M, Kressler J, Kammer HW. *Polymer* 1987;28:957–60.
- [9] Stein VDJ, Jung RH, Illers KH, Henders H. *Ankew Makromol Chem* 1974;36:89–100.
- [10] Cowie JMG, Lath D. *Makromol Chem, Macromol Symp* 1988;16:103–12.
- [11] Bernstein RE, Cruz CA, Paul DR, Barlow JW. *Macromolecules* 1977;10:681–6.
- [12] Kressler J, Kammer HW, Klostermann K. *Polym Bull* 1986;15:113–9.
- [13] Fowler ME, Barlow JW, Paul DR. *Polymer* 1987;28:1177–84.
- [14] Lyngaae-Jorgensen J, Sondergaard K. *Polym Engng Sci* 1987;27:351–8.
- [15] Subramanian R, Huang YS, Roach JF, Wiff DR. *Mater Res Soc Symp Proc* 1990;171:217–24.
- [16] Kammer HW, Kummerloewe C, Kressler J, Melior JP. *Polymer* 1991;32:1488–92.
- [17] McMaster LP. *Macromolecules* 1973;6(5):760–73.
- [18] Klotz S, Cantow HJ. *Polymer* 1990;31:315–22.
- [19] Chai ZK, Sun RN. *Polymer* 1983;24:263–70.
- [20] Walsh DJ, Higgins JS, Rostami S. *Macromolecules* 1983;16:391–6.
- [21] Rostami S, Walsh DJ. *Macromolecules* 1984;17:315–20.
- [22] Walsh DJ, Rostami S. *Polymer* 1985;26:418–22.
- [23] Shiomi T, Imai K. *Polymer* 1991;32(1):73–8.
- [24] Shiomi T, Ishimatsu H, Eguchi T, Imai K. *Macromolecules* 1990;23:4970–7. p. 4978–82.
- [25] Jo WH, Lee MS. *Macromolecules* 1992;25:842–8.
- [26] Sata T, Tohyama M, Suzuki M, Shiomi T, Imai K. *Macromolecules* 1996;29:8231–40.
- [27] Kammer HW, Kressler J, Scheller D, Kroschwitz H, Schmidnaake G. *Acta Polym* 1989;40(2):75–80.
- [28] Shimomai K, Higashida N, Ougizawa T, Inoue T. *Polymer* 1996;37(26):5877–82.
- [29] Flory PJ. *J Am Chem Soc* 1965;87:1833–7.
- [30] Eichinger BE, Flory PJ. *Trans Faraday Soc* 1968;65:2035–65.
- [31] Flory PJ, Orwoll RA, Vrij A. *J Am Chem Soc* 1964;86:3515–20.
- [32] Bondi AJ. *Phys Chem* 1964;68:441–55.
- [33] Choi K, Jo WH. *Macromolecules* 1997;30:1509–14.
- [34] Cowie JMG, Li GX, Ferguson R, McEwan IJ. *J Polym Sci: Part B: Polym Phys* 1992;30:1351–8.
- [35] Dudowicz J, Freed KF. *Macromolecules* 1998;31:5094–104.
- [36] Pavawongsak S. PhD Thesis. Imperial College, London; 1996.
- [37] Manda D. PhD Thesis. Imperial College, London; 1998.
- [38] Rojanapitayakorn P, Thongyai S, Higgins JS, Clarke N. *Polymer* 2001;42:3475–87.